Northumbria Research Link

Northumbria
University
NEWCASTLE

Unipolar-pulse amplitude modulation frequency division multiplexing for visible light communication systems

Osama Saied, [a, *] Zabih Ghassemlooy,[b] Stanislav Zvanovec,[c] Refik Caglar Kizilirmak,[d] Bangjiang Lin.[e]

[a]University of Gharyan, Department of Electrical and Electronic Engineering, Gharyan, Libya.
[b]Optical Communications Research Group, Faculty of Engineering and Environment, Northumbria University, UK.
[c]Czech Technical University in Prague, Department of Electromagnetic Field, Prague, Czech Republic.
[d]Nazarbayev University, Department of Electrical and Computer Engineering, Astana, Kazakhstan.
[a]Quanzhou Institute of Equipment Manufacturing, Haixi Institutes, Chinese Academy of Sciences, Quanzhou, China

Abstract. Asymmetrically clipped optical orthogonal frequency division multiplexing (ACO-OFDM) has been proposed in visible light communication (VLC) systems to overcome the DC-biased optical OFDM (DC-OFDM) power consumption issue at the cost of the available electrical spectral efficiency. Due to the implementation of inverse fast Fourier transform (IFFT), all the optical OFDM schemes including ACO-OFDM suffer from large peck to average power ratio (PAPR), which degrade the performance in VLC systems as the light emitting diodes used as the transmitter have a limited optical power-current linear range. To address the PAPR issue in ACO-OFDM, in this work we introduce a unipolar-pulse amplitude modulation frequency division multiplexing (U-PAM-FDM) by adopting the single carrier frequency division multiple access (SC-FDMA). This is achieved by considering a PAM as an SC-FDMA data symbols and inserting a conjugate copy of the middle and first SC-FDMA FFT output subcarriers after the middle and last subcarriers, respectively. Simulation results show that, for the proposed scheme the PAPR is 3.6 dB lower compared with ACO-OFDM. The PAPR improvement is further analyzed with the simulation results demonstrating that the proposed scheme offers 2.5 dB more average transmitted power compared to ACO-OFDM.

Keywords: SC-FDMA, ACO-OFDM, VLC, PAPR, LED, Dynamic range.

***First Author, E-mail: osama.dhawi.saied@hotmail.com

1 Introduction

Visible light communications (VLC) is a novel wireless technology that uses light emitting diode (LED)-based sources for the dual purpose of lighting and data communications [1, 2]. Unlike radio frequency (RF)-based systems, the light spectrum is unregulated, and VLC can use the entire or portions of the visible spectrum (385 - 790 THz) [1, 2]. Nevertheless, the transmission bandwidth in VLC systems is mostly limited by the modulation bandwidth of the LED B_{mod}. For example, the bandwidth of the standard high-power white phosphor LED (WPLED), which is used for illumination, is in the range of a few MHz [1, 2].

To address the LED's bandwidth limitation and therefore increase the transmission data rates, a few methods have been proposed in the literature. For example, the multiple-input multiple-output

(MIMO) technique, where higher capacity and diversity gain can be achieved using spatial multiplexing and repetition coding as compared with single-input single-output (SISO) systems [3]. MIMO has also been used together with multi-carrier transmission as in [4, 5], where the link capacity was improved using adaptive transmission in frequency selective channels. Additionally, in [6], optical blue filtering was applied at the receiver (Rx) to suppress the slow response of the phosphor whereas, the analogue pre- and post-equalization techniques were investigated in [7-9] to increase B_{mod} and consequently improve the VLC throughput. For instance, in [7] B_{mod} of the blue, red and green LEDs with the emitter degenerated LED driver was increased by (*i*) 106, 87 and 98 MHz, respectively using a pre-equalizer; and (*ii*) 174, 180 and 145 MHz, respectively based on the pre- and post-equalizers. However, the improvement in B_{mod} was achieved at the cost of reduced signal to noise ratio (SNR) per transmitted symbol at the Rx [10, 11].

Alternatively, to improve B_{mod}, non-orthogonal multiple access (NOMA) method was considered for multiple access channels [12, 13], where all the user terminals share the entire available bandwidth at the same time. In addition to the aforementioned techniques, multi-level modulation signal schemes including M-ary pulse amplitude modulation (M-PAM) have also been demonstrated to increase the data rate [14]. However, instead of single carrier modulation (SCM), a multi-carrier modulation (MCM) schemes such as orthogonal frequency division multiplexing (OFDM) have been adopted to boost the transmission data rate in VLC systems. For instance, in a recent demonstration [15], the data rate of more than 15 Gbps was reported using OFDM with optimum bit and power loading based on wavelength division multiplexing of four LEDs (i.e., RGBY). Although, OFDM has many promising benefits in VLC, traditional OFDM signal generation techniques used in RF systems cannot be directly applied to intensity modulation and direct detection (IM/DD)-based VLC systems. First and foremost, in IM/DD systems, the

information bearing signal should be non-negative and real valued. In the literature, the three most commonly used optical OFDM techniques are DC-biased optical OFDM (DCO-OFDM), asymmetrically clipped optical OFDM (ACO-OFDM) and pulse amplitude modulated discrete multitone (PAM-DMT), where all of which rely on Hermitian symmetry (HS) in the complex symbol vector prior to time domain signal generation through inverse fast Fourier transform (IFFT). HS ensures that, the signal at the output of IFFT is a real valued. In order to satisfy the non-negativity condition, DCO-OFDM systems add a DC bias before clipping the negative residual signal, whereas the even subcarriers (SCs) of ACO-OFDM and the real part of PAM-DMT data symbols are kept blank so that the negative amplitudes levels at the output IFFT of both schemes conveys no information and hence are clipped. As compared with RF systems, in IM/DD-based OFDM VLC transmission, the electrical spectral efficiency is halved for DCO-OFDM while it is reduced to one fourth in ACO-OFDM and PAM-DMT. However, ACO-OFDM and PAM-DMT are more optical power efficiency and have lower noise clipping compared with DCO-OFDM [16-20]. Due to inclusion of a number of SC components during IFFT operation, OFDM waveforms suffer from high peak to average power ratio (PAPR). This leads to several practical issues, which needs addressing such as the limited dynamic ranges of digital to analog converter (DAC) and electrical amplifiers. But particularly in VLC systems, the limited linear dynamic range of LED's optical power-current characteristics, which can lead to reduced PAPR and therefore distortions of the transmitted and received signals [21, 22]. In order to avoid high PAPR, instead of OFDM, single-carrier frequency division multiple access (SC-FDMA) was proposed in [23-25]. SC-FDMA is two types: localization frequency division multiple access (LFDMA) and interleaved frequency division multiple access (IFDMA), and is currently employed for the uplink multiple access schemes in the long term evolution (LTE) of cellular systems by the third generation

partnership project (3GPP) [26, 27]. ACO-single carrier frequency domain equalization (ACO-SCFDE) was proposed in [23] and [24] as a modified IFDMA scheme, which is suitable for IM/DD. The only difference between ACO-OFDM and ACO-SCFDE is the inclusion of FFT and IFFT blocks in the ACO-SCFDE transmitter (Tx) and ACO-SCFDE Rx, respectively. However, in order to meet IM/DD requirements, the IFDMA symbol vector in all these modified schemes, again needs to satisfy HS, which results in increased PAPR in optical-based IFDMA compared with RF-based IFDMA. In [25], it was demonstrated that, because of HS only half of the ACO-SCFDE samples would have a single carrier PAPR behavior, while the other half will have the same PAPR as in OFDM. However, in our recent work [28, 29], we showed that PAPR of optical IFDMA can be improved by not considering HS requirement and therefore making it to be as low as the PAPR of IFDMA in the RF domain. This was achieved in [29] by symmetrically repeating the IFDMA time domain symbol twice by means of setting the interleaving factor (Q) in the frequency domain to be 2. That is, the IFDMA symbol was transmitted through two sub symbols, where the real and imaginary parts of IFDMA time domain samples were transmitted using the 1st and 2nd sub symbols, respectively. However, for VLC systems, the 1st SC (i.e., the DC term) is used for keeping the LED on, dimming or shifting the amplitude levels within the dynamic range of LEDs [1, 2]. Because of the implementation of the interleaving mapping and FFT process at the Tx, the 1st SC in [28, 29] needs to be a modulated SC, which is affected by the DC bias and consequently affecting all samples in the time domain. Thus, resulting in 2 dB of SNR penalty compared with traditional optical OFDM to achieve the same bit error rate (BER) as demonstrated in [29].

In this paper, the unipolar-PAM frequency division multiplexing (U-PAM-FDM) signalling scheme for the IM/DD-based VLC system is introduced as a means to improve the PAPR of the

optical OFDM. This improvement is achieved by removing the requirement for HS in IFDMA and without any DC bias effects. Here, since we have adopted PAM as the data symbols (i.e., real values), the FFT SCs outputs at the IFDMA Tx are symmetrically conjugated, except for the first and the middle SCs. However, to make all SCs symmetrically conjugated, two additional SCs are included after the middle and the end of the FFT output, which we call it the symmetrically conjugate (SCG) process. Implementing odd modulation and IFFT on theses modified SCs results in a real and asymmetric signal suitable for IM/DD based VLC systems.

The paper is structured as follows; Section **2** presents the proposed U-PAM-FDM scheme. Results obtained for the proposed scheme are analyzed and evaluated in Section **3**. Finally, conclusions are drawn in Section **4**.

2 U-PAM-FDM System Description

In this section, we outline details of the Tx and the Rx for U-PAM-FDM.

2.1 U-PAM-FDM Tx

Fig. 1 depicts the block diagram of the U-PAM-FDM Tx. An input random serial binary bit stream *bi* is first converted into the parallel bit streams prior to being mapped to PAM. The generated output signal $C = \{C_0, C_1, C_2, C_3 \dots \dots C_{D-1}\}$, where D is the number of transmitted data symbols, which is a real vector, is applied to the FFT module with the output of which given by:

$$S_m = \sum_{d=0}^{M-1} c_d \, e^{\frac{-j2\pi dm}{M}}, \quad \textbf{(1)}$$

where $S = \{S_0, S_1, S_2, \dots \dots S_{M-1}\}$, M is the FFT size, which is equal to D, and m and d are the m^{th} SC and d^{th} data symbol, respectively.

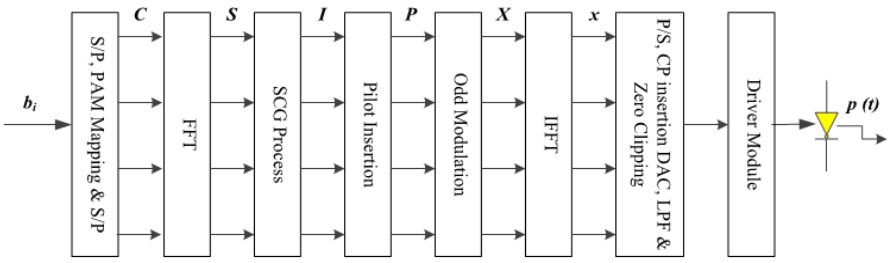

Fig. 1 The block diagram of the U-PAM-FDM Tx.

Since C is a real signal (i.e., PAM), all SCs at the output of FFT are symmetrically conjugated around the $S_{\left(\frac{M}{2}+1\right)}$ SC except the S_0, see Fig. 2. Note, the m^{th} SC is given as:

$$\begin{aligned} S_m &= \sum_{d=0}^{M-1} C_d \; e^{-j2\pi dm/M}, \\ S_{M-m} &= \sum_{d=0}^{M-1} C_d \; e^{-j(2\pi dm/M)(M-m)}, \\ &= \sum_{d=0}^{M-1} C_d \; e^{-j(2\pi m-(2\pi dm/M))}, \\ &= \sum_{d=0}^{M-1} C_d \; e^{j(2\pi dm/M)}. \end{aligned} \tag{2}$$

S_0	S_1	S_2	S_3	S_4	S_3^*	S_2^*	S_1^*

Fig. 2 The SCs for eight real input samples at the output of FFT module.

From (2) and Fig. 2, it can be clearly observed that each m^{th} SC is conjugated with the $(M-m)^{th}$ SC (i.e., $S_m = S^*_{M-m}$), since C is composed of real values. However, in order to obtain an asymmetric real time domain signal, which is the requirement for IM/DD VLC links, all the SCs must be symmetrically conjugated (i.e., $S_m = S^*_{M-m+1}$) by then to apply to the SCG block, where two additional SCs (i.e., $S^*_{\left(\frac{M}{2}+1\right)} = S^*_4$ for M = 8 and S^*_0) are included to S after the centre and the last SCs. The SCG output vector, which is illustrated in Fig. 3, is given by:

$$I = \{I_0, I_1, I_2, I_3, \ldots\ldots I_{Z-1}\},$$

$$I = \left\{S_0, S_1, \dots, S_{\frac{M}{2}}, S_{\left(\frac{M}{2}+1\right)}, S^*_{\left(\frac{M}{2}+1\right)}, S^*_{\frac{M}{2}}, \dots S^*_1, S^*_0\right\}, \quad \textbf{(3)}$$

where $Z = M + 2$.

S_0	S_1	S_2	S_3	S_4	S^*_4	S^*_3	S^*_2	S^*_1	S^*_0

Fig. 3 The frequency domain SCs at the output of the SCG module for *M*=8 and *Z*=10.

For the purpose of channel estimation, a number of symmetrically conjugate pilots are inserted to *I* as depicted in Fig. 4 and is given by:

$$P = \{P_0, P_1, P_2, P_3, \dots \dots P_{V-1}\}, \quad \textbf{(4)}$$

$\boldsymbol{P_0}$	I_0	I_1	I_2	$\boldsymbol{P_1}$	I_3	I_4	I_5	I_6	$\boldsymbol{P^*_1}$	I_7	I_8	I_9	$\boldsymbol{P^*_0}$

Fig. 4 The frequency domain SCs with pilot signals for *Z*=10 and *A* = 4

where $V = Z + A$ and *A* is the number of pilots, which depends on the channel characterization. *P* is subsequently applied to the odd modulation and IFFT modules the outputs of which are given by, respectively:

$$\begin{aligned} X &= \{X_0, X_1, X_2 \dots \dots, X_{T-1}\}, \\ &= \{0, P_0, 0, P_1, 0, P_2 \dots \dots, 0, P_{Z-1}\}, \end{aligned} \quad \textbf{(5)}$$

$$x_n = \frac{1}{N}\sum_{k=0}^{N-1} X_k \, \mathrm{e}^{\frac{2\pi nk}{N}}, \quad \textbf{(6)}$$

where $T = 2V$, *N* is the IFFT points, and *n* and *k* are the n^{th} time domain sample of *x* and the k^{th} frequency domain SC of *X*, respectively. Note that, the output of the IFFT is now a real asymmetric signal. Finally, as in the traditional ACO-OFDM scheme, *x* is applied to the parallel to serial (P/S), a cyclic prefix (CP), DAC, low pass filter (LPF) and zero clipping module prior to IM of the LED via the driver unit.

2.1 U-PAM-FDM Rx

Fig. 5 shows the schematic block diagram of the U-PAM-FDM Rx. Following optical detection, the received signal is given by:

$$y(t) = r(t) + w\,(t), \tag{7}$$

where the regenerated electrical signal $r(t) = Rp(t) * h(t)$, R is the responsivity of the photodetector (PD), which is assumed to be unity in this work, $p(t)$ is the transmitted optical signal, symbol * denote the linear convolution , $h(t)$ is the impulse response of the system and $w(t)$ represents the shot (signal and ambient light) and terminal noise sources, which are modelled as the additive white gaussian noise (AWGN). $y(t)$ is then passed through the LPF, analog digital converter (ADC) and CP removal modules prior to being converted to the frequency domain *Y* using the FFT. Subsequently, the redundant SCs (i.e., the even SCs) are removed from *Y* and the resulting signal *YC* is applied to the pilot extraction block to recover the pilot symbols (*YP*) for channel estimation. The received random data symbols *YD* together with the estimated transfer function of the system $\widehat{H}$ are applied to a single-tab zero forcing equalizer (ZFE) with the output given by:

$$YE = \frac{YD}{\widehat{H}}. \tag{8}$$

Finally, YE is applied to the IFFT and PAM de-mapping blocks in order to generate the estimated data stream.

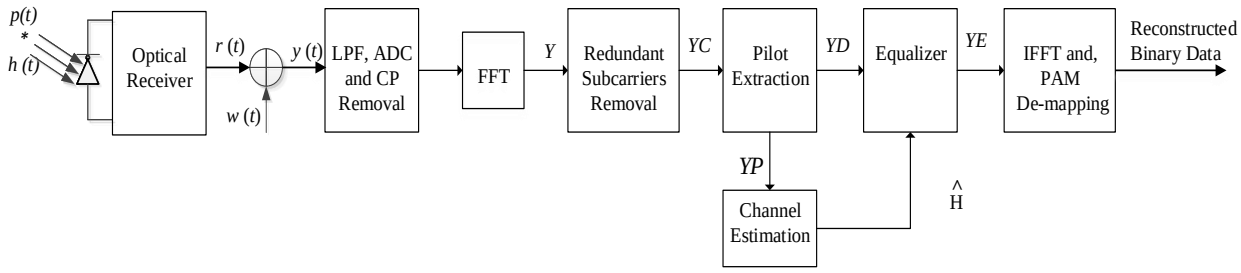

Fig. 5 The block diagram of the U-PAM-FDM Rx

3 Results and Analysis

In this section, the simulation results for the performance of the U-PAM-FDM scheme are presented. We consider 256 IFFT points and a CP with a duration of 50 ns, which is the maximum time delay for the multipath indoor VLC channel [30]. A 1 W white LED with PCB (HPB8-49KxWDx) is used with a 1 V quasi-linear dynamic range where its measured L-I-V curve is illustrated in Fig. 6.

To obtain an optimum comparison between U-PAM-FDM, ACO-OFDM and ACO-SCFDE in terms of the SNR, BER and EVM, the PAM symbols of U-PAM-FDM are generated at the Tx by separating the real and the imaginary parts of QAM symbols (i.e., the ($a + bj$) QAM symbol is separated into 'a' and 'b' PAM symbols), where these symbols are combined together at the Rx to reconstruct the QAM. All the key parameters adopted for simulation are given above in Table I.

Table 1 Key simulation parameters.

Parameter	**Value**
Number of iterations	1 M
LED Type	1W white LED with PCB (HPB849KxWDx)
LED bandwidth	2MHz
LED linearity	$\sim 1\ V$
The distance between LED and PD	2 m
LED half-power angle $\emptyset_{1/2}$	70^0
Photodetector (PD)	Thorlab (PDA36A-EC) [31].
PD gain	0 dB
PD bandwidth	10 MHz
PD noise (RMS)	300 µV
PD responsivity	0.65 A/W
PD active area	16 mm^2
Rx FOV	180^0

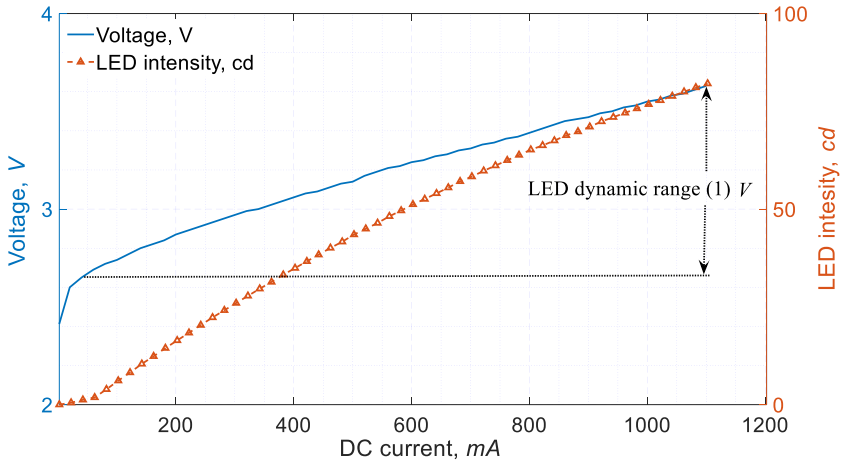

Fig. 6 Measured L-I-V curves of the 1 W white LED (HPB8-49KxWDx) (Northumbria university research Lab)

The probability of the PAPR being higher than a certain threshold level (i.e., PAPR_0) are illustrated in Figs. 7 and 8 where, as in [32-34], a complementary cumulative distribution function (CCDF) of 10^{-4}, i.e.$Pr\{\mathrm{PAPR} > \mathrm{PAPR}_0\} = 0.0001$, is considered.

Fig. 7 illustrates the CCDF as a function of the PAPR for the ACO-OFDM, ACO-SCFDE and U-PAM-FDM schemes where, ACO-OFDM has higher PAPR values by ~3.6 and ~2.1 dB compared with U-PAM-FDM and ACO-SCFDE, respectively. The PAPR improvement of the ACO-SCFDE and U-PAM-FDM schemes are due to the insertion of the FFT and the interleaving mapping (i.e., odd modulation) blocks prior to IFFT at the OFDM Tx. Note by doing so, OFDM PAPR is as low as the SCM scheme reported in [27]. However, in IM/DD ACO-SCFDE and U-PAM-FDM VLC systems, the HS and SCG blocks should be implemented following FFT at the Tx, which leads to increased PAPR compared with the SCM scheme, since not all SCs enjoy the mapping feature.

Next, we investigated the effect of pilot insertion on the PAPR for ACO-OFDM, ACO-SCFDE and U-PAM-FDM and compared them with no pilot cases, as illustrated in Fig. 8. The plots shown clearly demonstrate that, at CCDF of 10^{-4} ACO-SCFDE and U-PAM-FDM with 8 pilots (i.e. A = 8, where A is the number of pilots) have higher PAPRs by 0.4 and 0.9 dB, respectively, compared with the cases with no pilot symbols. For A = 16 based ACO-SCFDE and U-PAM-FDM the

increase in PAPRs are 0.6 and 1.3 dB, respectively, where the insertion of the pilots has no impact on the ACO-OFDM PAPR. These increases of the PAPR for ACO-SCFDE and U-PAM-FDM are due to the insertion of pilot symbols, which change the order of the SCs, thus reducing the number of SC benefiting from the mapping feature. However, the insertion of pilots may not be required in VLC systems, since the indoor channel is highly stable and deterministic, which can be estimated once and then adopted for the incoming symbols.

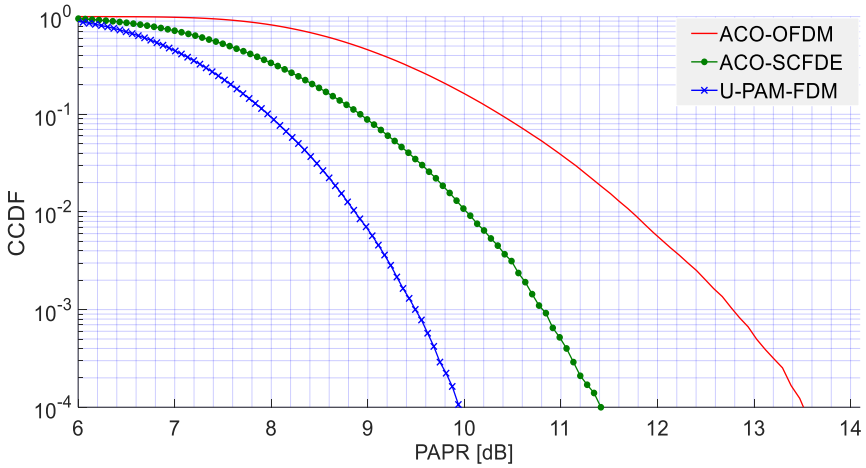

Fig. 7 CCDF vs. PAPR for ACO-OFDM, ACO-SCFDE and U-PAM-FDM

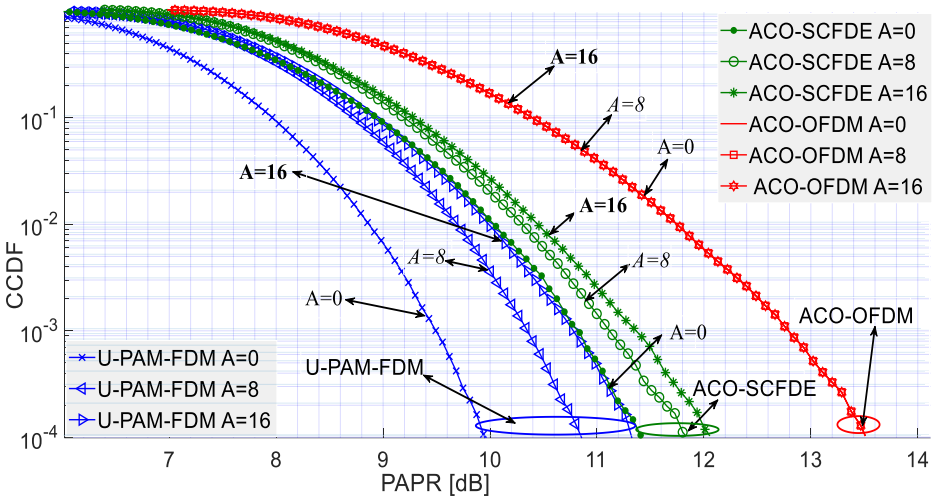

Fig. 8 CCDF vs. PAPR for ACO-OFDM, ACO-SCFDE and U-PAM-FDM with and without the pilot symbols where A is the number of pilots.

Finally, the impact of PAPR on the performance of VLC is numerically investigated by considering the limited LED power-current dynamic range, as was discussed earlier. Since the OFDM schemes have different PAPR values, their transmit average electrical power (P_{avg}) reaches the maximum value of the LED dynamic linear range (L_{D_Max}) i.e., clipping level at different dBm values, which can be obtained from the error vector magnitude (EVM).

Fig. 9 shows the EVM as a function of P_{avg} for the 16- and 256-QAM ACO-OFDM, ACO-SCFDE and U-PAM-FDM schemes for the average noise power ${\sigma_n}^2$ of -10 dBm. As illustrated in Fig. 9, the EVM reduces by increasing P_{avg}, reaching the minimum level (i.e. reaching L_{D_Max}) at 18 < P_{avg} < 21 dBm depending on the OFDM schemes where the best EVM performance is achieved for U-PAM-FDM as it has the lowest PAPR value. However, after these P_{avg} values, the EVM start increasing as the system performance starts affected by the clipping noise where the maximum achievable average electrical power is obtained when EVM reaches its threshold values. According to [35, 36] for 16- and 256-QAM, the EVM threshold values should be ≤ 12.5% and 3.5%, respectively. As such for 16-QAM U-PAM-FDM provide 2.5- and 1-dB higher P_{avg} than ACO-ODM and ACO-SCFDE schemes, respectively. However, for 256 QAM none of these schemes reach the EVM threshold level as they require a wider LED dynamic linear range (i.e., >1 *V*). Note increasing the order of QAM for the same scheme have no impact on the L_{D_Max}.

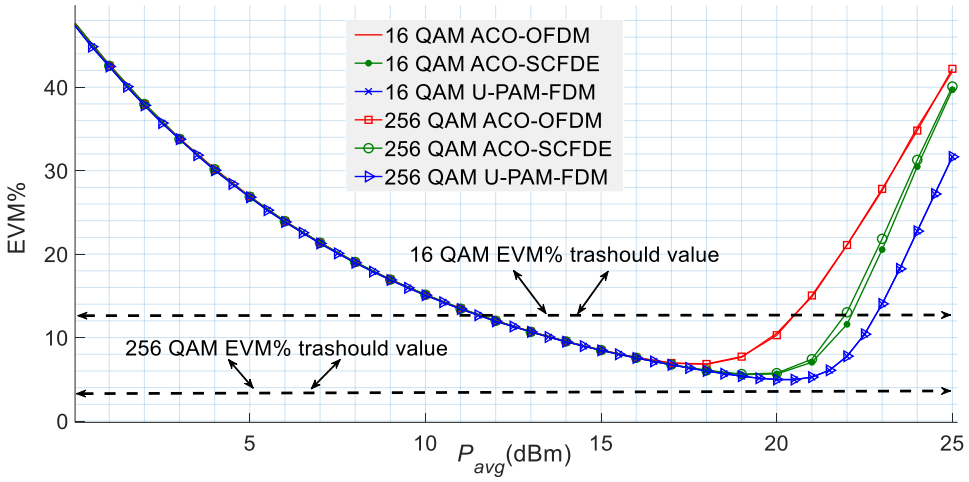

Fig. 9 EVM vs P_{avg} for 16- and 256-QAM ACO-OFDM, ACO-SCFDE and U-PAM-FDM

Next, we investigate the effect of the clipping noise on the BER performance as a function of P_{avg} for 16-, 64- 128-, and 256-QAM ACO-OFDM, ACO-SCFDE and U-PAM-FDM and for ${\sigma_n}^2$ of -10 dBm, as depicted in Fig. 10. These plots illustrate that, the proposed scheme outperforms ACO-OFDM and ACO-SCFDE for all QAM constellation orders because of the lowest PAPR value. Fig. 10 (a) shows that, although ACO-OFDM has a higher PAPR value compared with ACO-SCFDE, it outperforms ACO-SCFDE at lower order QAM signals (i.e., $\leq$ 16-QAM), This is because, ACO-OFDM distributed time domain samples provide lower clipping noise, which can be reduced at the Rx using soft and hard decision methods when lower QAM is considered.

However, for higher order QAM signals, even the low clipping noise cannot be treated at the Rx and therefore, for > 16 QAM constellation order, the scheme with lower PAPR will provide improved BER performance as can be easily observed from Fig. 10 (b) where the U-PAM-FDM scheme provides the best BER performance while ACO-OFDM has the worst one.

Finally, Fig. 11, shows the distribution of 100 k time domain samples of ACO-OFDM, ACO-SCFDE and U-PAM-FDM. From the figure, one can observe that, most of the ACO-OFDM time domain samples are distributed around the mean value (i.e., zero value), where the number of

samples with large amplitudes for ACO-OFDM is low compared with the other two schemes, which results in a lower number of clipped samples (i.e., lower clipping noise). This explains why ACO-OFDM outperform ACO-SCFDE for lower QAM constellation orders (i.e,. ≤ 16-QAM) as was illustrated in Fig. 10 (a). Note, although the time domain samples of U-PAM-FDM and ACO-SCFDE have almost the same distribution, U-PAM-FDM outperforms ACO-OFDM for all QAM constellation orders, because of its lowest PAPR value as was already discussed.

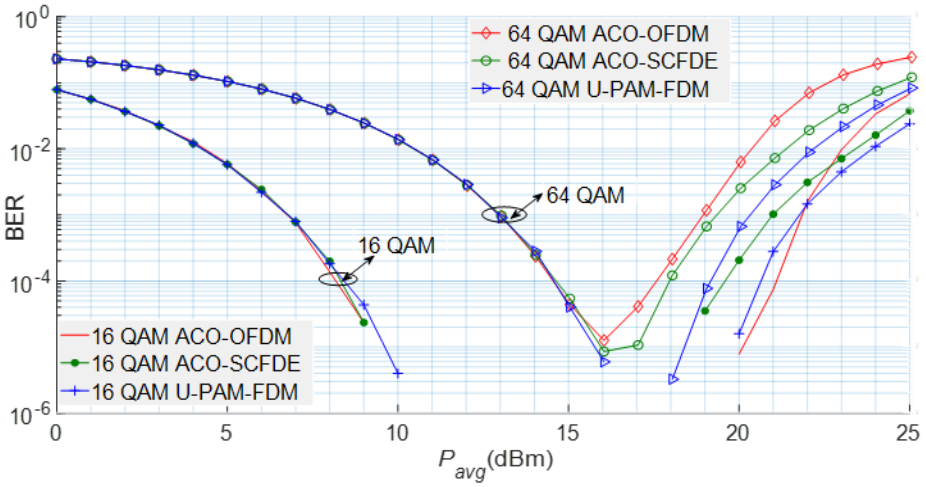

(a)

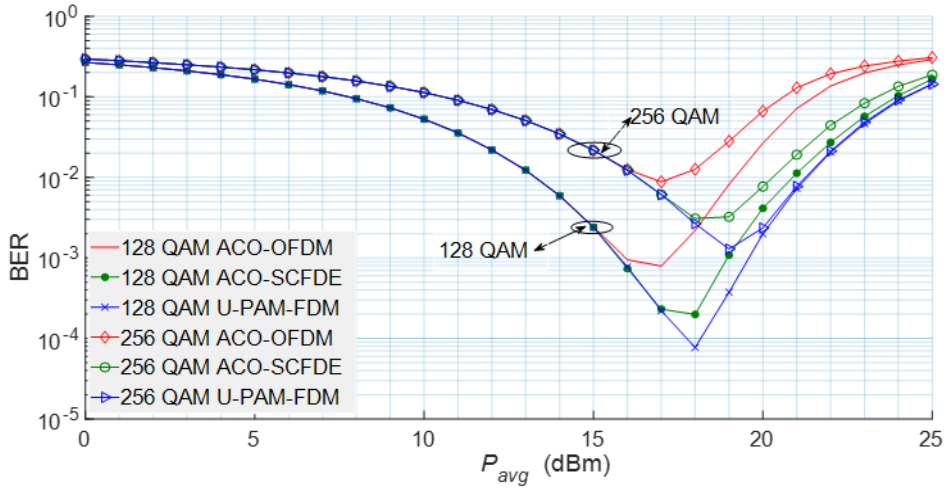

(b)

Fig. 10 The BER as a function of P_{avg} for ACO-OFDM, SCFDE, and UPAM-FDM with: (a) 16- and 64-QAM and (b) 128- and 256-QAM

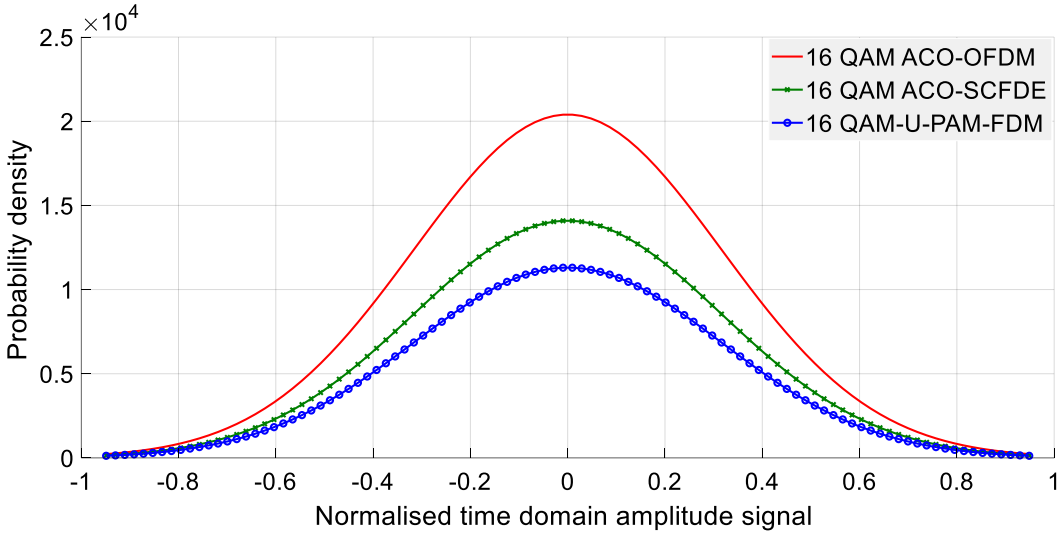

Fig. 11 Normal distribution function for ACO-OFDM, ACO-SCFDE and U-PAM-FDM data symbols

4 Conclusion

We introduced a new unipolar PAM-FDM scheme in order to reduce PAPR of unipolar optical OFDM by modifying SC-FDMA for used in IM/DD-based VLC. For U-PAM-FDM, the simulation results showed that the PAPR values are 3.6 and 1.5 dB lower compared with ACO-OFDM and ACO-SCFDE, respectively. We also investigated the impact of reducing PAPR on the EVM performance and showed that U-PAM-FDM offered higher P_{avg} by 2.5 dB compared with the traditional ACO-OFDM scheme.

References

1. Hoeher, Peter Adam. *Visible Light Communications: Theoretical and Practical Foundations*, Carl Hanser Verlag GmbH Co KG (2019).
2. Ghassemlooy Zabih, et al, *Visible light communications: theory and applications*, CRC press, (2017).
3. T. Fath and H. Haas, "Performance Comparison of MIMO Techniques for Optical Wireless Communications in Indoor Environments, " *IEEE Transactions on Communications*, **61**, (2), pp 733-742, (2013) [doi 10.1109/TCOMM.2012.120512.110578].

4. Y. Hong, T. Wu and L. Chen, "On the Performance of Adaptive MIMO-OFDM Indoor Visible Light Communications, " *IEEE Photonics Technology Letters*, **28,** (8), pp. 907 – 910, (2016) [doi:10.1109/LPT.2016.2517192].

5. O. Narmanlioglu, R. C. Kizilirmak, T. Baykas and M. Uysal, "Link Adaptation for MIMO OFDM Visible Light Communication Systems, " *IEEE Access*, **5**, pp. 26006– 26014, (2017) [doi: 10.1109/ACCESS.2017.2771333].

6. Shao-Wei Wang, et al, "A high-performance blue filter for a white-led-based visible light communication system," *IEEE wireless communications*, **22** (2), pp. 61–67 (2015) [doi:10.1109/MWC.2015.7096286].

7. Fujimoto, Nobuhiro, and Shohei Yamamoto. "The fastest visible light transmissions of 662 Mb/s by a blue LED, 600 Mb/s by a red LED, and 520 Mb/s by a green LED based on simple OOK-NRZ modulation of a commercially available RGB-type white LED using pre-emphasis and post-equalizing techniques," *The European Conference on Optical Communication (ECOC)*, pp. 1-3, IEEE, Cannes, France, (2014) [doi:10.1109/ECOC.2014.6963895].

8. X. Huang, Z. Wang, J. Shi, Y. Wang, and N. Chi, "1.6 Gbit/s phosphorescent white LED based VLC transmission using a cascaded pre-equalization circuit and a differential outputs PIN receiver," *Opt. Express*, **23** (17), pp. 22034–22 042, (2015) [doi:https://doi.org/10.1364/OE.23.022034].

9. H. Li, X. Chen, J. Guo, and H. Chen, "A 550 Mbit/s real-time visible light communication system based on phosphorescent white light LED for practical high-speed low-complexity application," *Opt. Express*, **22** (22), pp. 27203-27213, (2014) [doi:https://doi.org/10.1364/OE.22.027203].

10. P. A. Haigh, Z. Ghassemlooy, S. Rajbhandari, I. Papakonstantinou and W. Popoola, "Visible Light Communications: 170 Mb/s Using an Artificial Neural Network Equalizer in a Low Bandwidth White Light Configuration," *Journal of Lightwave Technology*, **32** (9), pp. 1807-1813, (2014) [doi:10.1109/JLT.2014.2314635].

11. X. Li, Z. Ghassemlooy, S. Zvanovec, R. Perez-Jimenez and P. A. Haigh, "Should Analogue Pre-Equalisers be Avoided in VLC Systems?" *IEEE Photonics Journal*, **12** (2), pp. 1-14, (2020) [doi:10.1109/JPHOT.2020.2966875].

12. H. Marshoud, S. Muhaidat, P. C. Sofotasios, S. Hussain, M. A. Imran and B. S. Sharif, "Optical Non-Orthogonal Multiple Access for Visible Light Communication, " *IEEE Wireless Communications*, **25**, (2), pp. 82–88, (2018) [doi:10.1109/MWC.2018.1700122].

13. C. Chen, W. Zhong, H. Yang and P. Du, "On the Performance of MIMO-NOMA-Based Visible Light Communication Systems, " *IEEE Photonics Technology Letters*, **30** (4), pp. 307-310, (2018) [doi: 10.1109/LPT.2017.2785964].

14. M. Wolf and M. Haardt, "On the DC balance of multi-level PAM VLC systems," *21st International Conference on Transparent Optical Networks (ICTON)*, pp. 1-5, IEEE, Angers, France, (2019) [doi:10.1109/ICTON.2019.8840531].

15. R. Bian, I. Tavakkolnia and H. Haas, "15.73 Gb/s Visible Light Communication with Off-the-Shelf LEDs," *Journal of Lightwave Technology*, **37** (10), pp. 2418-2424, (2019) [doi:10.1109/JLT.2019.2906464].

16. J. Armstrong and A. J. Lowery, "Power efficient optical OFDM," *Electronics Letters*, **42** (6), pp. 370-372, (2006) [doi:10.1049/el:20063636].

17. S. C. J. Lee, S. Randel, F. Breyer and A. M. J. Koonen, "PAM-DMT for Intensity-Modulated and Direct-Detection Optical Communication Systems," *IEEE Photonics Technology Letters*, **21** (23), pp. 1749-1751, (2009) [doi:10.1109/LPT.2009.2032663].

18. O. Saied, et al, "Position encoded asymmetrically clipped optical orthogonal frequency division multiplexing in visible light communications, " *Journal of Communications and Information Networks* **2** (4), pp. 1–10, (2017) [doi:org/10.1007/s41650-017-0038-2].

19. M. P. S. Bhadoria, G. Pandey and A. Dixit, "Performance Evaluation of Visible Light Communication for DCO and ACO Optical OFDM Techniques," *National Conference on Communications (NCC)*, pp. 1-6, IEEE, Bangalore, India, (2019) [doi:10.1109/NCC.2019.8732220].
20. Saied, Osama, et al. "Pilot-aided asymmetrically clipped optical OFDM in visible light communication," *The mediterranean journal of electronics and communications*, **12** (2), pp. 64-71, 2016.
21. T. Q. Wang, H. Li and X. Huang, "Analysis and Mitigation of Clipping Noise in Layered ACO-OFDM Based Visible Light Communication Systems," *IEEE Transactions on Communications*, **67** (1), pp. 564-577, (2019) [doi:10.1109/TCOMM.2018.2868665].
22. W. Hu, "PAPR Reduction in DCO-OFDM Visible Light Communication Systems Using Optimized Odd and Even Sequences Combination," *IEEE Photonics Journal*, **11** (1), pp. 1-15, (2019) [doi:10.1109/JPHOT.2019.2892871].
23. R. Mesleh, "OFDM and SCFDE performance comparison for indoor optical wireless communication systems, " *19th International Conference on Telecommunications (ICT)*, pp. 1–5, IEEE, Jounieh, Lebanon (2012) [doi:10.1109/ICTEL.2012.6221267].
24. Acolatse, Kodzovi, Yeheskel Bar-Ness, and Sarah Kate Wilson. "Novel techniques of single-carrierfrequency-domain equalization for optical wireless communications," *EURASIP Journal on Advances in Signal Processing*, pp. 1-13. [doi:https://doi.org/10.1155/2011/393768].
25. C. Wu, H. Zhang, W. Xu, "On visible light communication using LED array with DFT-spread OFDM, " *IEEE International Conference on Communications (ICC)*, pp. 3325-3330, IEEE, Sydney, Australia, (2014) [doi:10.1109/ICC.2014.6883834].
26. Zyren, Jim, and Wes McCoy. "Overview of the 3GPP long term evolution physical layer," *Freescale Semiconductor, Inc*, white paper 7, pp. 2-22 (2007).
27. H. G. Myung, L. Junsung, and D. Goodman, "Peak-To-Average Power Ratio of Single Carrier FDMA Signals with Pulse Shaping," *17th International Symposium on Personal, Indoor and Mobile Radio Communications*, pp. 1-5, IEEE, Helsinki, Finland, (2006) [doi:10.1109/PIMRC.2006.254407].

28. O. Saied, et al., ‘’Single carrier optical FDM in visible light communication,’’ *10th International Symposium on Communication Systems, Networks and Digital Signal Processing (CSNDSP)*, pp. 1–5, IEEE, Prague, Czech Republic (2016) [doi:10.1109/CSNDSP.2016.7573947].
29. Saied, Osama, et al. ‘’Optical single carrier-interleaved frequency division multiplexing for visible light communication systems,’’ *Optik*, **194**, pp. 162910 (2019) [doi:https://doi.org/10.1016/j.ijleo.2019.06.010].
30. S. Dimitrov and H. Haas, *Principles of LED Light Communications: Towards Networked Li-Fi*: Cambridge University Press, (2015).
31. THORLABS. (2006). PDA36A-EC - Si Switchable Gain Detector, 350-1100 nm, 10 MHz BW,13 mm2, M4 Taps Available: https://www.thorlabs.com/catalogpages/obsolete/2018/PDA36AEC.pdf
32. T. Zhang, H. Ji, Z. Ghassemlooy, X. Tang, B. Lin and S. Qiao, " Spectrum-Efficient Triple-Layer Hybrid Optical OFDM for IM/DD-Based Optical Wireless Communications, " *IEEE Access*, **8**, pp. 10352-10362, (2020) [doi: 10.1109/ACCESS.2020.2964792].
33. J. G. Doblado, A. C. O. Oria, V. Baena-Lecuyer, P. Lopez and D. Perez-Calderon, " Cubic Metric Reduction for DCO-OFDM Visible Light Communication Systems, " *Journal of Lightwave Technology*, **33** (10), pp. 1971-1978, (2015) [doi: 10.1109/JLT.2015.2402755].
34. N. Taşpınar and M. Yıldırım, " A Novel Parallel Artificial Bee Colony Algorithm and Its PAPR Reduction Performance Using SLM Scheme in OFDM and MIMO-OFDM Systems, " *IEEE Communications Letters*, **19** (10), pp. 830-1833, (2015) [doi: 10.1109/LCOMM.2015.2465967].
35. X. Liu, F. Effenberger, N. Chand, Z. Lei, and L. Huafeng, ‘’Demonstration of bandwidth-efficient mobile fronthaul enabling seamless aggregation of 36 E-UTRA-like wireless signals in a single 1.1-GHz wavelength channel,’’ *Optical Fiber Communications Conference and Exhibition (OFC)*, pp. 1-3, IEEE, Los Angeles, USA (2015).
36. Haibo Li, et al., ‘’Improving performance of mobile fronthaul architecture employing high order delta-sigma modulator with PAM-4 format,’’ Optics express, 25 (1), pp. 1-9, (2017) [https://doi.org/10.1364/OE.25.000001].

Osama Saied *Received his higher diploma (Hons.) degree in electronic engineering from the High Institute for Poly Technics, Gharyan, Libya in 2000, worked as networking engineering from 2001 to 2008 in Biruni Remote Sensing Center (BRSC) Tripoli, Libya. He received his M.Sc. degree in communication and signal processing in 2010 from University of Newcastle upon Tyne, UK. He got his PhD in visible light communications at Northumbria University, Newcastle upon Tyne, UK in 2018. He has published 4 journal papers and one conference paper. His research interests include optical wireless communications, free space optics, visible light communications and RF over optics.*

Zabih Ghassemlooy *Received the B.Sc. (Hons.) degree in electrical and electronics engineering from Manchester Metropolitan University, U.K., in 1981, and the M.Sc. and Ph.D. degrees from the University of Manchester, U.K., in 1984 and 1987, respectively. He is currently pursuing the C.Eng. degree. From 1987 to 1988, he was a Postdoctoral Research Fellow with the City, University of London, U.K. In 1988, he joined Sheffield Hallam University as a Lecturer, where he became a Professor, in 1997. In 2004, he joined the University of Northumbria, Newcastle upon Tyne, as the Associate Dean (AD) of research with the School of Engineering. From 2012 to 2014, he was the AD of the Research and Innovation, Faculty of Engineering and Environment, where he is currently the Head of the Optical Communications Research Group. He has published over 850 articles (330 journals and eight books). His research interests include optical wireless communications, free space optics, visible light communications, radio over fibre-free space optics, and sensor networks with project funding from EU, U.K. Research Council and industry.*

Stanislav Zvanovec *Received the M.Sc. and Ph.D. degrees from the Czech Technical University in Prague in 2002 and 2006, respectively, where he is a Full Professor, the Deputy Head of the Department of Electromagnetic Field, and a Leader of Wireless and Fiber Optics Team. He has*

authored two books and more than 250 journal articles and conference papers. His current research interests include FSO and fiber optical systems, VLC, and RF over optics.

Bangjiang Lin *Received the B.Sc. and M.Sc. degrees in Electrical and Electronics Engineering from Bilkent University, Ankara, Turkey, in 2004 and 2006, respectively, and the Ph.D. degree from Keio University, Yokohama, Japan, in 2010. He worked for the Communications and Spectrum Management Research Center, Turkey, on several telecommunication and defense industry projects. He contributed to the technical requirements document of 802.15.7r1 standardization, which will enable VLC. He has three patent applications in the field of wireless communications to US and Japan patent offices. Currently, he is with the Department of Electrical and Electronics Engineering, Nazarbayev University, Astana, Kazakhstan. He is the recipient of IEEE VTS Japan 2008 Young Researcher's and IEICE WBS Best Paper Awards.*

Bangjiang Lin *Received the B.Sc. and the Ph.D. degrees from the Electronics Engineering Department, Peking University, Beijing, China, in 2010 and 2015, respectively. He joined with the Quanzhou Institute of Equipment Manufacturing, Haixi Institutes, Chinese Academy of Sciences, in 2015, as a Lecturer, where he became an Associate Professor, in 2017. He has published more than 100 articles of which half are SCI indexed. His current research interests include passive optical networks and visible light communications.*